



# Abrupt changes in Great Britain vegetation carbon projected under climate change

Chris A. Boulton | Paul D. L. Ritchie | Timothy M. Lenton

Global Systems Institute, College of Life and Environmental Sciences, University of Exeter, Exeter, UK

## Correspondence

Chris A. Boulton, Global Systems Institute, College of Life and Environmental Sciences, University of Exeter, Exeter EX4 4QE, UK.  
Email: c.a.boulton@exeter.ac.uk

## Funding information

Natural Environment Research Council, Grant/Award Number: NE/P007880/1; Leverhulme Trust, Grant/Award Number: RPG-2018-046

## Abstract

Past abrupt 'regime shifts' have been observed in a range of ecosystems due to various forcing factors. Large-scale abrupt shifts are projected for some terrestrial ecosystems under climate change, particularly in tropical and high-latitude regions. However, there is very little high-resolution modelling of smaller-scale future projected abrupt shifts in ecosystems, and relatively less focus on the potential for abrupt shifts in temperate terrestrial ecosystems. Here, we show that numerous climate-driven abrupt shifts in vegetation carbon are projected in a high-resolution model of Great Britain's land surface driven by two different climate change scenarios. In each scenario, the effects of climate and CO<sub>2</sub> combined are isolated from the effects of climate change alone. We use a new algorithm to detect and classify abrupt shifts in model time series, assessing the sign and strength of the non-linear responses. The abrupt ecosystem changes projected are non-linear responses to climate change, not simply driven by abrupt shifts in climate. Depending on the scenario, 374–1,144 grid cells of 1.5 km × 1.5 km each, comprising 0.5%–1.5% of Great Britain's land area show abrupt shifts in vegetation carbon. We find that abrupt ecosystem shifts associated with increases (rather than decreases) in vegetation carbon, show the greatest potential for early warning signals (rising autocorrelation and variance beforehand). In one scenario, 89% of abrupt increases in vegetation carbon show increasing autocorrelation and variance beforehand. Across the scenarios, 81% of abrupt increases in vegetation carbon have increasing autocorrelation and 74% increasing variance beforehand, whereas for decreases in vegetation carbon these figures are 56% and 47% respectively. Our results should not be taken as specific spatial or temporal predictions of abrupt ecosystem change. However, they serve to illustrate that numerous abrupt shifts in temperate terrestrial ecosystems could occur in a changing climate, with some early warning signals detectable beforehand.

## KEYWORDS

abrupt shift, climate change, temperate ecosystem, tipping point, vegetation carbon

This is an open access article under the terms of the Creative Commons Attribution License, which permits use, distribution and reproduction in any medium, provided the original work is properly cited.

© 2020 The Authors. *Global Change Biology* published by John Wiley & Sons Ltd

## 1 | INTRODUCTION

Tipping points, where a small change makes a big difference to the state and/or fate of a system, can occur in a variety of complex systems including the climate system (Lenton et al., 2008) and ecosystems (Scheffer, Carpenter, Foley, Folke, & Walker, 2001). More broadly, abrupt changes—where a system responds much faster than it is forced—can occur in the climate (Alley, 2000; Alley et al., 2003) and ecosystems (Ratajczak et al., 2018). Catastrophic shifts are a subset of abrupt changes, which are large and inherently difficult to reverse, as they involve tipping points between alternative stable states. Evidence of abrupt change in the climate system has been found in both palaeo-records (Alley, 2000) and general circulation model projections of future climate change (Drijfhout et al., 2015). Past abrupt changes have also been observed in a range of aquatic and terrestrial ecosystems due to a range of forcing factors, including pollution, land-use change and over-exploitation of populations (Scheffer, 2009). Climate change may already have contributed to abrupt shifts in terrestrial ecosystems, notably widespread forest dieback, including due to bark beetle outbreaks in the Canadian boreal forest (Bentz et al., 2010; Kurz et al., 2008) and increased wildfires preventing forest regeneration (Davis et al., 2019). There is a widespread expectation that future climate change poses a threat to many species and could cause abrupt changes in some ecosystems (Ibáñez et al., 2006; Ratajczak et al., 2018; Thomas et al., 2004).

At the relatively large spatial scale of global climate model projections, multiple abrupt shifts have been found in parts of the physical climate system and in some biomes, mostly in the tropics and polar regions (Drijfhout et al., 2015). Candidates include possible abrupt shifts in tropical forest-savannah systems and boreal forest-tundra systems (Lenton et al., 2008). The potential for large-scale abrupt shifts in temperate terrestrial ecosystems is less recognized—either in the historical record or in future projections—perhaps because the strength of feedback coupling to the atmosphere is generally weaker than in the tropics and high latitudes. However, at smaller spatial scales, more localized self-amplifying feedbacks can propel abrupt change (Lenton, 2013)—for example, involving disturbance factors such as pest infestation (Kurz et al., 2008) or fires (Hirota, Holmgren, Van Nes, & Scheffer, 2011; Staver, Archibald, & Levin, 2011) and/or interactions between vegetation types, even positive ones (Kéfi, Holmgren, & Scheffer, 2016)—potentially across all latitudes. Furthermore, threshold behaviour (rather than positive feedback) can lead to abrupt shifts—notably drought thresholds for temperate forest dieback (Allen et al., 2010; Hoffman, Marchin, Abit, & Lau, 2011).

That said, high-resolution, process-based modelling of climate change-driven abrupt shifts in ecosystems is limited. Hence we set out to examine whether a state-of-the-art land surface and ecosystem model run at high resolution over GB, under different climate change scenarios, would show abrupt changes or linear response to climate forcing. Current thinking is that GB peatlands are most vulnerable to abrupt disappearance under climate

change (Gallego-Sala & Prentice, 2012), but the model we use does not represent peatlands well; so our focus instead is on lowland woodlands and grasslands. There are few previous suggestions of climate change driving abrupt shifts in these GB ecosystems, and those that exist focus on forest dieback in one location (Evans et al., 2017; Martin, Newton, Cantarello, & Evans, 2017), making the spatial extent of our results surprising. The results here complement previous studies of temperate aquatic systems that are well known to exhibit abrupt shifts, which in that case are also catastrophic (Carpenter & Kinne, 2003; Scheffer et al., 2001; Scheffer & Jeppesen, 2007). Our definition of abruptness here does not require a shift to be large in magnitude or irreversible, just anomalous in rate. Furthermore, we consider whether abrupt increases in vegetation could be triggered, particularly by CO<sub>2</sub> fertilization. Our results also help inform consideration of changes in vegetation carbon stores in national carbon accounting, and proposals in the UK to plant more trees to remove atmospheric CO<sub>2</sub>.

## 2 | MATERIALS AND METHODS

We drove the Joint UK Land Environment Simulator (JULES) with different climate change projections and then analysed the output with a novel, automated abrupt change detection algorithm (Boulton & Lenton, 2019).

### 2.1 | Climate scenarios

For UK climate change scenarios, we use two different perturbed parameter configurations of the HadRM3-PPE-UK model (Hadley Centre for Climate Prediction & Research, 2014), run under the same SRES A1B 'balanced' climate forcing scenario from 1998 to 2100. This perturbed physics ensemble (PPE) was designed to simulate UK regional climate change as part of the 'UK-Climate Projections' project (UKCP09; Murphy et al., 2009). PPEs are used to explore uncertainty in parameters that control the physical processes within the model by perturbing them within experts' opinions of their ranges. Here, we use the standard, unperturbed run which has an equivalent climate sensitivity of 3.5K globally and another that is more sensitive, having a climate sensitivity of 7.1K globally—noting that this does not necessarily mean that a proportionally larger temperature increase is found within the UK. These runs consist of daily data at a 25 km × 25 km spatial resolution which has been spatially interpolated to a 1.5 km × 1.5 km resolution for use in the land surface model (detailed below).

### 2.2 | JULES runs and variables

JULES is the land surface model component of the UK Met Office's Unified Model (Best et al., 2011; Clark et al., 2011). It

calculates fluxes of CO<sub>2</sub>, heat, water and momentum between the land surface and atmosphere, and models five plant functional types (PFTs; Broadleaf and Needleleaf trees, C3 and C4 grasses, and shrubs) using the TRIFFID vegetation model (Cox, 2001; Cox et al., 2001). Photosynthesis and plant respiration are calculated for each PFT, and then the fractional coverage of each plant type within a grid box is updated. Competition between plant types is simulated using Lotka–Volterra-type equations. Key equations detailing carbon uptake and allocation within a plant type are given in Appendix S1. JULES has been shown to perform well at simulating vegetation globally when compared with observations (Harper et al., 2018). We use an agricultural land mask to partition part of each grid box such that trees cannot grow in areas set aside for farming. This land mask is created from land-use data derived from the June Agricultural Census (JAC) panel from EDINA (agcensus.edina.ac.uk) at 2 km × 2 km resolution. Land use does not change over the simulation. JULES is run at 1.5 km × 1.5 km resolution with GB comprising 77,980 land grid boxes.

For each of the two different climate change scenarios, we undertake a run of fixed, 'present day' level (386.5 ppm) CO<sub>2</sub> and a run with changing CO<sub>2</sub> corresponding to the SRES A1B scenario, leading to four different runs of JULES. A recent study has shown that significant greening in a quarter of Earth's vegetated areas over the last 35 years is due to rising atmospheric CO<sub>2</sub> levels (Zhu et al., 2016). Thus these different CO<sub>2</sub> pathways allow us to explore how the CO<sub>2</sub> fertilization effect, where increased atmospheric CO<sub>2</sub> increases photosynthesis whilst reducing evapotranspiration, affects the number of abrupt shifts we find. Our analysis focuses on total vegetation carbon (C<sub>veg</sub>) per grid box (kg/m<sup>2</sup>) as initial analysis showed evidence of abrupt shift behaviour (see below). To ensure that the abrupt shifts we detect are not due to abrupt shifts in the driving data, we also focus on rainfall (mm/day) and surface temperature (°C). In these climate data, we look for both abrupt shifts and potential thresholds that may have caused this behaviour in C<sub>veg</sub>.

### 2.3 | Abrupt shift detection

Our method to detect abrupt shifts in time series is based around searching for anomalous rates of change in a system (i.e. the gradient of the time series) over time. We give a brief overview here but more detail can be found elsewhere (Boulton & Lenton, 2019). We begin by separating the time series into sections of a predetermined length, *l*, and then fit linear regression models through each section. An anomalous rate of change is defined as a gradient that is more than three median absolute deviations away from the median gradient. Wherever this occurs in time it is recorded by adding or subtracting (depending on which direction the anomaly was in) a value of 1 from a 'detection times series' that is the same length as the original time series. This process is repeated for a range of section lengths, *l*, from a lower bound up to a length less than or equal to

one third of the total length of the time series (such that there are a minimum of three segments used). We then divide the 'detection time series' by the number of lengths used, giving the proportion that a time point was considered part of an abrupt shift.

We run our abrupt shift detection algorithm over annually averaged data (101 years), with *l* spanning from 5 to 33 years in incremental steps of 1 and use the maximum absolute value of the abrupt shift detection time series to determine if an abrupt shift has occurred. We use annual data for detecting abrupt shifts as this is computationally efficient. However we use monthly data when calculating potential early warning signals in those time series that exhibit abrupt shifts, as there are not enough data to detect a signal in the annual data.

Because the maximum absolute value of the detection time series can be influenced by factors such as the amplitude of noise in the time series tested, we determine a threshold value by ranking time series by their maximum detection value and randomly observing C<sub>veg</sub> time series with certain maximum detection values. From this, we deduced that a threshold of 0.4 is appropriate to detect an abrupt shift, that is, at least 40% of the window lengths used detected an anomalous gradient at the specific time point. We focus only on the most strongly detected abrupt shift within a time series for this analysis, even if there is more than one abrupt shift detected in a given time series.

### 2.4 | Abrupt shift classification

We detected a number of distinct types of shift in the time series data which we have classified. First we separate out time series with abrupt shifts within the first 20 years, from those where they occur later. Abrupt shifts that were detected in the first 20 years are classed as 'start'. They are necessarily hard to predict using early warning signals and may have little to do with future climate change, and more to do with imperfect initialization of the model. Furthermore, by using a lowest *l* of 5 years in the detection algorithm, if a maximum rating is found within the first 20 years, most of the time the maximum detection is found in the first year.

We determine if the time series has increased or decreased overall by comparing the means of the first and last 10 years. For those time series where the abrupt change is found after the first 20 years, and is in the same direction as the overall change of the time series, we call these 'traditional' abrupt shifts as they follow the typical pattern of abrupt shifts in ecosystems. If the abrupt shift is in the opposite direction (e.g. there is growth overall but an abrupt downwards shift), we call these 'against' abrupt shifts.

Our algorithm detects a flat section in an otherwise increasing or decreasing time series. We filter out time series that have these flat sections detected in them. To find them we compare the gradient of a regression model fitted on 20 years centred on the detected shift with the final full time series. If the gradient around the detected shift is smaller than the full time series we consider a flat section has been detected. All of the flat sections

were detected at the start of the time series, with an increase or decrease afterwards.

The combinations of factors above give rise to six classes of detected abrupt shift (AS), relative to the overall trend (D):

- Traditional: Overall increase, abrupt shift positive (T:  $D > 0$ ,  $AS > 0$ )
- Traditional: Overall decrease, abrupt shift negative (T:  $D < 0$ ,  $AS < 0$ )
- Against: Overall increase, abrupt shift negative (A:  $D > 0$ ,  $AS < 0$ )
- Against: Overall decrease, abrupt shift positive (A:  $D < 0$ ,  $AS > 0$ )
- Start: Negative abrupt shift (S:  $AS < 0$ )
- Start: Positive abrupt shift (S:  $AS > 0$ )

All time series can be classified as long as they are not constant with a small 'spike' within, which would cause the overall growth/decline to be 0. This only occurs in grid boxes that contain no vegetation carbon but a small rounding error causes a negligible spike for a single year in the time series. However, by setting a threshold for detection, these types of series can be disregarded. We note that our 20 year boundary for determining an abrupt shift at the start could be separating classes that are caused by the same dynamics. However, we separate them because when calculating early warning indicators, we need at least 20 years' worth of data.

## 2.5 | Early warning indicators

We test for early warning signals consistent with tipping point dynamics on the 'traditional' abrupt shifts detected in the  $C_{veg}$  time series, by searching for critical slowing down (Scheffer et al., 2009). We note that abrupt shifts can have a number of causes and only some are due to a weakening of negative feedbacks before a positive feedback takes over at a tipping point—that is, the phenomenology that causes critical slowing down. Hence, this search for tipping point early warning signals can be viewed as one way of trying to establish the nature of the underlying dynamics of the detected abrupt shifts. We look for an increasing AR(1) (the lag-1 autocorrelation) and variance signal over time in monthly data, which can be indicators of critical slowing down occurring, first by removing the mean annual cycle, and then detrending each time series with a Kernel smoothing function with a bandwidth of 250. We use monthly data for measuring these indicators as we need more time points than we would have using only annual data. AR(1) and variance are calculated on a moving window equal to 20 years which moves across the time series 1 month at a time to create a time series of each indicator (Dakos et al., 2008; Held & Kleinen, 2004). Trends of each indicator are measured using a Mann–Kendall test (Dakos et al., 2008), a rank correlation test with one variable being time and the other the indicator. A Mann–Kendall  $\tau$  of 1 means the time series of the indicator is always increasing,  $-1$  always decreasing and 0 no overall trend.

## 3 | RESULTS

### 3.1 | Changes in climate over the century

We begin by looking at changes in the inputted climate variables (rainfall and temperature) in each forcing configuration. The starting climate (over the first 10 years) and difference at the end of the model runs (last 10 years) are shown in Figure 1. For rainfall changes, there is no difference between those from the constant  $CO_2$  runs and those from the A1B  $CO_2$  runs under the same climate sensitivity. However, there are small differences in surface temperature changes due to feedbacks between the vegetation and the atmosphere. In particular,  $CO_2$  fertilization causing stomatal closure reduces evapotranspiration. Hence, Figure 1 shows future changes in temperature from both constant  $CO_2$  and increased  $CO_2$  configurations.

The starting rain for the 3.5K sensitivity configuration (Figure 1a) shows that the west is wetter than the east, with the most rain occurring in the north-west, on the Scottish coastline. This pattern is more extreme for the 7.1K sensitivity configuration (Figure 1b), with a greater south-to-north gradient than is observed under 3.5K sensitivity. Over the century, an increase in rainfall is observed in the north-west but a decrease in the south-east in the 3.5K configuration (Figure 1c). This is also observed in the 7.1K configuration (Figure 1d), but the area of drying is smaller.

Starting temperatures show similar patterns for the two climate sensitivities (Figure 1e,f), with the 7.1K configuration being generally warmer. We see warmer surface temperatures in the southeast and in urban areas, notably London. Cooler temperatures are found in the north and north-west. Changes in temperature in all the configurations (Figure 1g–j) show warming everywhere, which is strongest in the south-east and weakest in the north-west.

### 3.2 | Changes in vegetation carbon ( $C_{veg}$ ) over the century

Over the first 10 years, there are only small differences in  $C_{veg}$  between our two  $CO_2$  configurations, hence starting  $C_{veg}$  is only shown for the constant  $CO_2$  configurations (Figure 2). We find similar patterns in  $C_{veg}$  for the 3.5K (Figure 2a) and 7.1K (Figure 2b) configurations; the majority of grid boxes have a  $C_{veg}$  of between 0.1 and 2  $kg/m^2$ , mostly C3 grasses (Figure S1). Values of  $C_{veg}$  less than 0.1  $kg/m^2$  relate mainly to urban areas and mountainous regions in the north. There are areas of higher  $C_{veg}$  found throughout Great Britain, which relate to broadleaf tree forests (Figure S1). More noticeable in the south, the starting  $C_{veg}$  of the 3.5K configuration is higher in the broadleaf tree areas (those with the higher  $C_{veg}$ ; Figure S1) than in the 7.1K configuration. We reiterate that the growth of vegetation, specifically trees, is limited to certain areas due to the land mask applied to our model runs.

For each forcing configuration, we analyse the change in  $C_{veg}$  over the century by comparing the mean  $C_{veg}$  in the final 10 years to the first 10 years (Figure 3). When considering the effects of

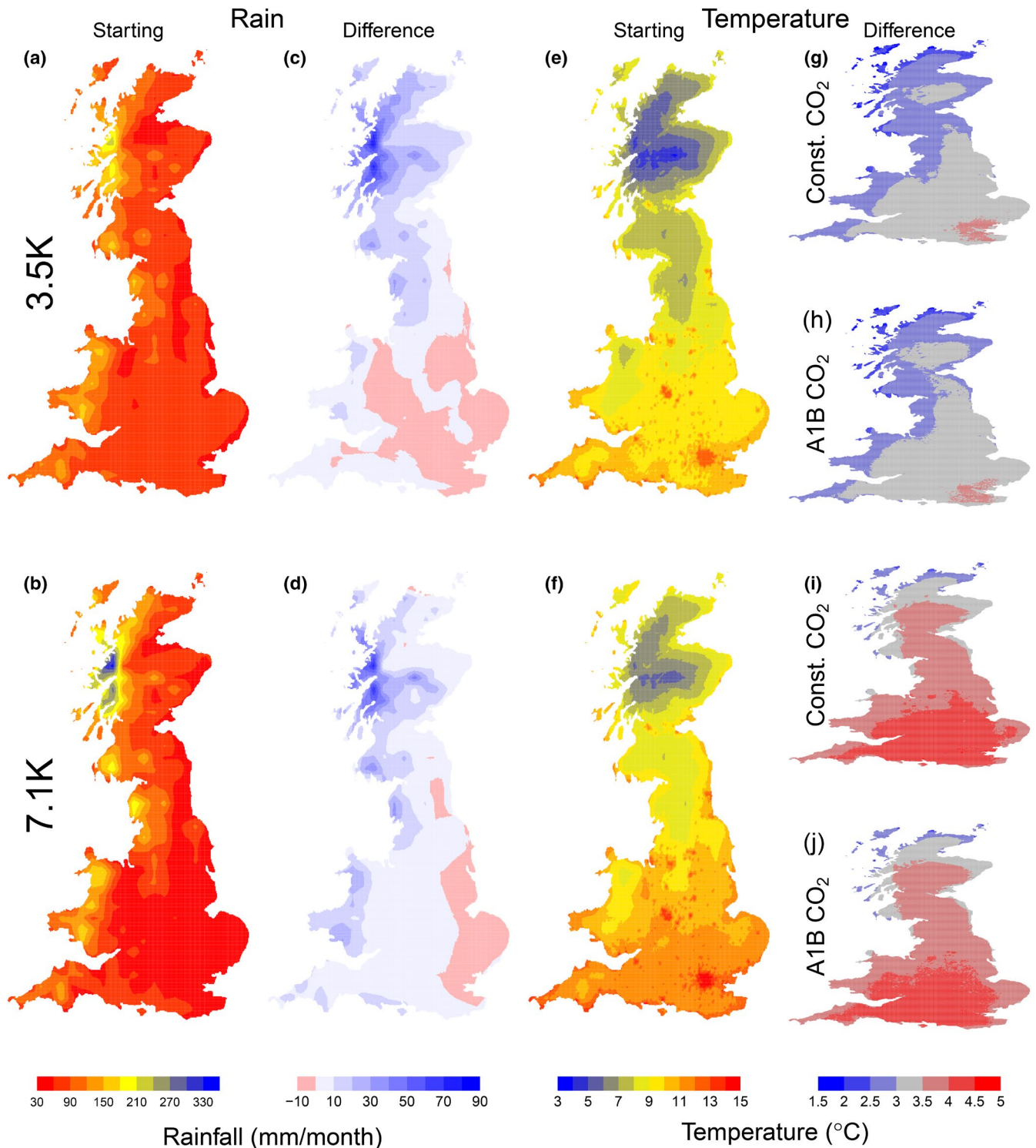


**FIGURE 1** Starting climate and change in climate for different global climate sensitivities (3.5K; 7.1K) and with/without CO<sub>2</sub> effects on vegetation: (a, b) initial rainfall averaged over 1998–2007; (c, d) change in rainfall averaged over 2089–2098 (identical for constant CO<sub>2</sub> and A1B CO<sub>2</sub>); (e, f) initial surface temperature (1998–2007); (g–j) change in surface temperature with (g, i) fixed CO<sub>2</sub>; (h, j) A1B CO<sub>2</sub> averaged over 2089–2098

climate change alone (i.e. keeping CO<sub>2</sub> at constant present day levels), for both climate sensitivities (3.5K; Figure 3a and 7.1K; Figure 3c) we find a mixture of increases and decreases in C<sub>veg</sub> over the century. Most losses occur in the south east, extending further north in the 7.1K sensitivity run (Figure 3c). However,

there are also 'hotspots' of C<sub>veg</sub> loss found in the north in the 3.5K sensitivity run (Figure 3a).

When CO<sub>2</sub> is allowed to increase following the A1B pathway with an associated fertilization effect on vegetation, we find increases in C<sub>veg</sub> nearly everywhere under both 3.5K (Figure 3b) and 7.1K (Figure 3d)

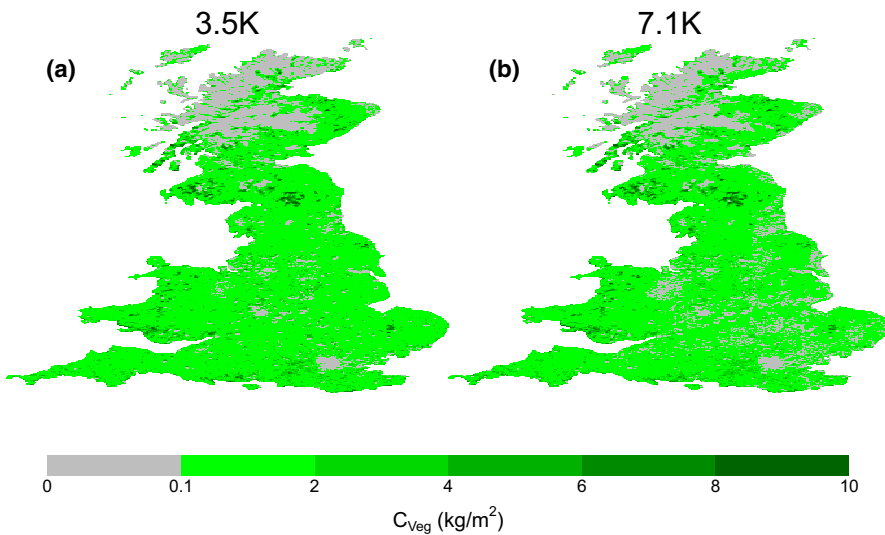


**FIGURE 2** Starting (mean of first 10 years: 1998–2007)  $C_{veg}$  values for the (a) 3.5K and (b) 7.1K constant  $CO_2$  configurations

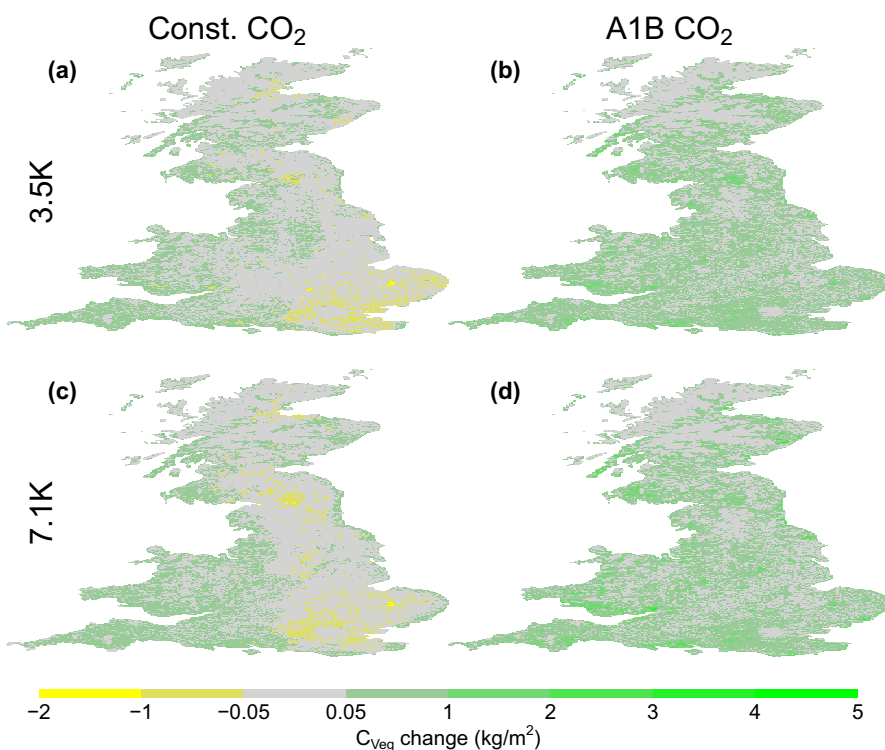


**FIGURE 3** Projected changes in  $C_{veg}$  (last 10 years: 2089–2098, compared with starting 10 years: 1998–2007) for the (a) 3.5K, constant  $CO_2$ , (b) 3.5K, A1B  $CO_2$ , (c) 7.1K, constant  $CO_2$ , and (d) 7.1K, A1B  $CO_2$  configurations

climate sensitivities. Thus, in this model, increases in  $CO_2$  can increase vegetation biomass in areas where temperature increases would otherwise cause dieback and loss of carbon. Note that there is no change in  $C_{veg}$  in areas such as London or Birmingham because there is very little vegetation to begin with (Figure 2) and it is unable to grow due to the fractional area of these grid boxes made up of mainly urban.

### 3.3 | Examples of classes of abrupt change

We use the 3.5K, constant  $CO_2$  configuration to illustrate all the types of abrupt change classified in Section 2. Figure 4 shows typical examples of time series that were classified as each type (using a

threshold in the detection time series of 0.4). Our 'traditional' abrupt shifts (Figure 4a,b) are well defined, while our 'against' examples (Figure 4c,d) show clear sharp, temporary changes in the direction of  $C_{veg}$  given its overall change. Our algorithm classifies time series based on the strongest abrupt change observed. For example, in the case of our increasing abrupt shift in an otherwise decreasing  $C_{veg}$  (Figure 4d), one may argue that there is another increasing abrupt shift near the end. However this one is less prominent than the one we focus on. Decreasing and increasing abrupt shifts found at the beginning (within the first 20 years; Figure 4e,f) show what is most likely spin-up problems with the model, that is, the original starting point of the variables in the model did not quite match the climate and the model reacted quickly to the sudden forcing. Whether or

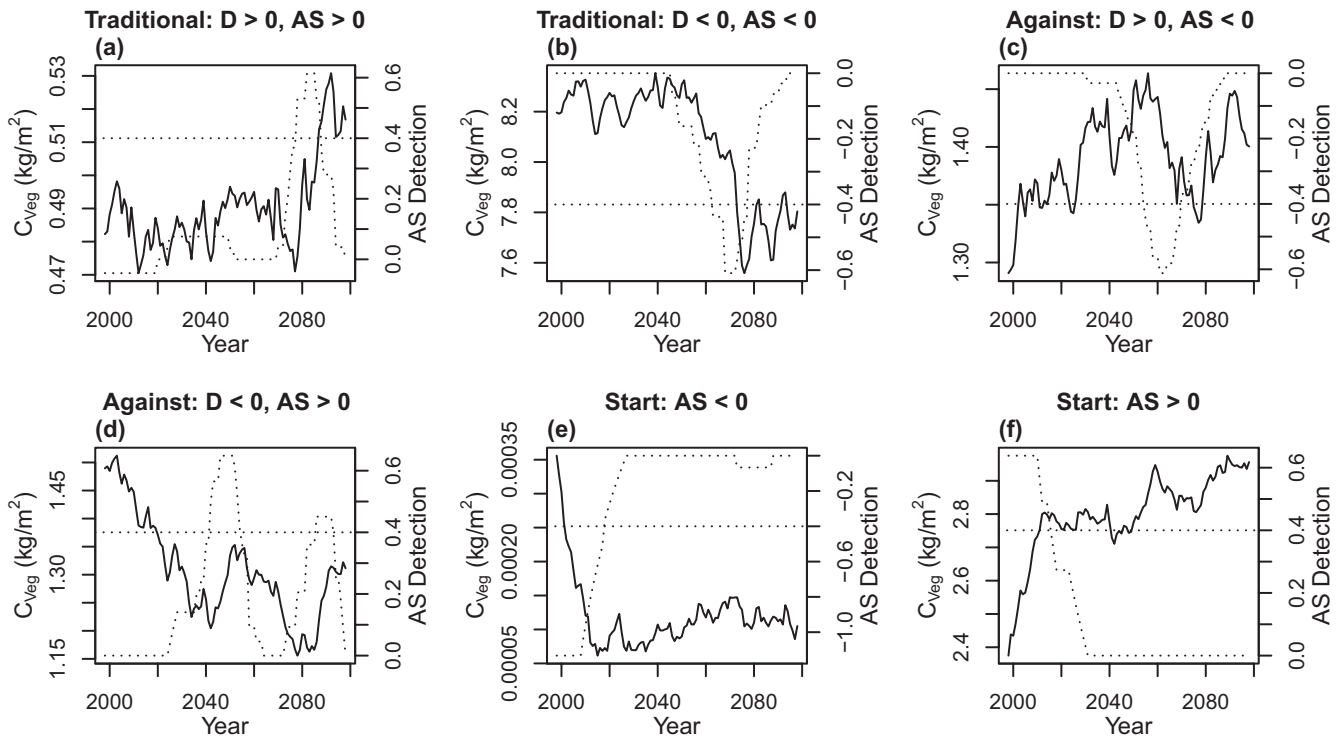


**FIGURE 4** Examples of  $C_{\text{Veg}}$  abrupt shift classes found in the 3.5K, constant  $\text{CO}_2$  configuration of JULES. Typical examples are shown of (a) Traditional:  $D > 0$ ,  $AS > 0$ , (b) Traditional:  $D < 0$ ,  $AS < 0$ , (c) Against:  $D > 0$ ,  $AS < 0$ , (d) Against:  $D < 0$ ,  $AS > 0$ , (e) Start:  $AS < 0$ , (f) Start:  $AS > 0$ . Explanations of these labels can be found in the main text. Solid black lines show the time series of the vegetation carbon and the dotted lines, the corresponding detection time series. Dotted horizontal lines refer to a detection of  $\pm 0.4$ , above (or below  $-0.4$ ) this a time series will be flagged as having an abrupt shift

not this is the cause, we exclude these in our analysis of early warning indicators as there are not enough data to calculate them on before the abrupt shift. We note that the absolute values of  $C_{\text{Veg}}$  in the decreasing abrupt shift at the start time series (Figure 4e) are very small but these are filtered out as results in the next section and only shown here for illustrative purposes.

### 3.4 | Spatial distribution of abrupt shifts

We now look at the spatial distribution of these classes of abrupt shift. Figure 5 shows the  $C_{\text{Veg}}$  abrupt shift classifications of grid boxes where the maximum detection was greater than 0.4. We also remove those grid boxes where the change in  $C_{\text{Veg}}$  across the abrupt shift (the difference between the mean  $C_{\text{Veg}}$  for the 5 years after the abrupt shift and the 5 years before) is less than  $0.01 \text{ kg/m}^2$  as we assume such small shifts are less ecologically interesting and would be hard to spot in reality. We discuss the range in sizes of abrupt shifts later on.

In the 3.5K constant  $\text{CO}_2$  run (Figure 5a), we find areas in the Scottish Highlands and East Midlands that contain decreasing abrupt shifts, regardless of whether  $C_{\text{Veg}}$  is increasing or decreasing overall (red and dark green). We also find areas of increasing abrupt shifts in otherwise decreasing  $C_{\text{Veg}}$  (orange) around the south-east of England. Scattered upland areas in Wales and Scotland showed abrupt  $C_{\text{Veg}}$  shifts at the start (blue and purple).

By introducing varying, A1B  $\text{CO}_2$  to the 3.5K run (Figure 5b), the majority of abrupt shifts can now be found in south-east England, north of London, in the form of increasing abrupt shifts in increasing  $C_{\text{Veg}}$  time series (light green). There are a number of starting shifts found on the England–Wales border, with much less found in Scotland than with the constant  $\text{CO}_2$ . We also find less decreasing abrupt shifts in Scotland than with the constant  $\text{CO}_2$ .

In the 7.1K, constant  $\text{CO}_2$  run (Figure 5c), we still find areas of decreasing abrupt shifts (red and dark green) in Scotland, but they do not necessarily match up with those areas found in the 3.5K, constant  $\text{CO}_2$  run. There are also regions of increasing abrupt shifts in generally increasing  $C_{\text{Veg}}$  (light green) found on the east and north-west Scottish coasts. These are also now found around the coast of Wales and in various places in the south-west of England. Concentrated areas of starting abrupt shifts can be found in the extreme south of Cornwall and Devon, as well as spaced around the south and midlands of England.

Less specific areas can be picked out in the 7.1K, A1B  $\text{CO}_2$  run (Figure 5d), with the main finding being increasing abrupt shifts in increasing  $C_{\text{Veg}}$  (light green) around the coasts of Scotland and Wales, as well as in central Scotland.

These results are summarized in Table 1. Surprisingly, the higher global climate sensitivity simulation generally shows fewer abrupt shifts in GB than the lower climate sensitivity simulation. Less surprisingly, for a given climate sensitivity there are fewer abrupt shifts

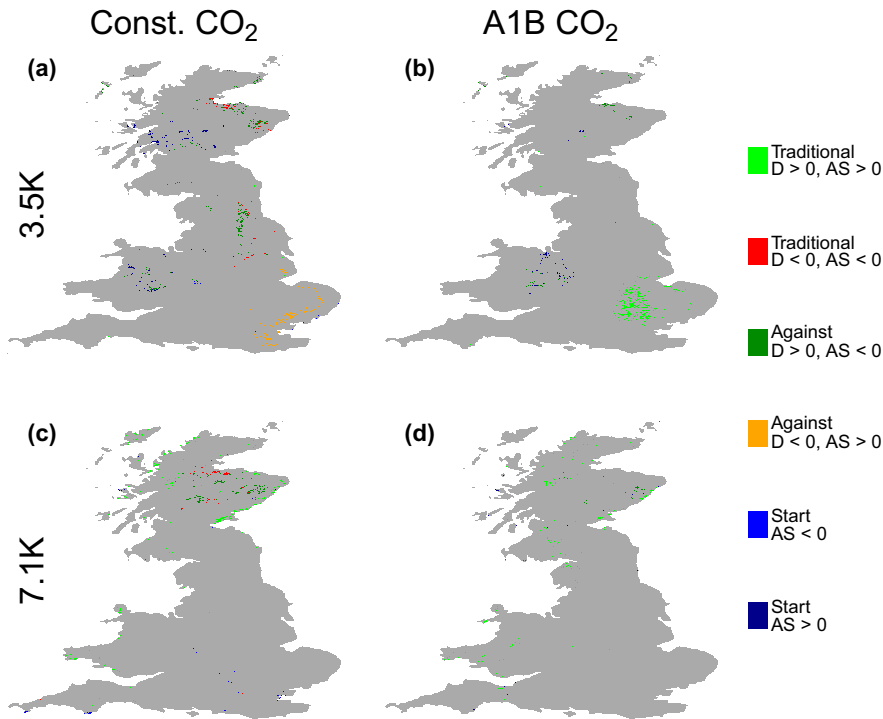


**FIGURE 5** Abrupt shift classifications for grid box  $C_{veg}$  in configurations (a) 3.5K, constant  $CO_2$ , (b) 3.5K, A1B  $CO_2$ , (c) 7.1K, constant  $CO_2$  and (d) 7.1K, A1B  $CO_2$ . Grid boxes are coloured grey if there is no detection rating above 0.4

	3.5K		7.1K	
	Const. $CO_2$	A1B $CO_2$	Const. $CO_2$	A1B $CO_2$
Traditional D > 0, AS > 0	13	545	474	296
Traditional D < 0, AS < 0	143	0	91	0
Against D > 0, AS < 0	434	108	225	41
Against D < 0, AS > 0	290	0	0	0
Start AS < 0	22	0	60	0
Start AS > 0	242	112	9	37
Total	1,144 (1.5%)	765 (1.3%)	859 (1.1%)	374 (0.5%)

**TABLE 1** The number of the 77,980 land grid boxes in each JULES configuration that were classified as each abrupt shift type with a detection rating greater than 0.4

under increasing A1B  $CO_2$  than constant  $CO_2$ . Traditional type decreasing abrupt shifts disappear in the increasing A1B  $CO_2$  runs, presumably because predicted overall declines in  $C_{veg}$  become very rare. With rising A1B  $CO_2$  there is an overall increase in number of grid boxes that have abrupt shifts associated with growth generally, whether they be at the start or not (T: D > 0, AS > 0, S: AS > 0), presumably because predicted overall increases in  $C_{veg}$  become more widespread.

### 3.5 | Abrupt shifts in the climate time series

To determine whether or not the abrupt shifts observed in  $C_{veg}$  are due to nonlinear behaviour and not a linear response to a nonlinear

change in the drivers, we ran the same analysis on the climate time series (rainfall and surface air temperature).

Using the annual time series of both the rainfall and temperature time series and the same detection threshold as for  $C_{veg}$  of 0.4, we only find a single time series (one spatial location) that has an abrupt shift: an 'against', decrease in temperature in an overall increasing temperature for the 3.5K, A1B  $CO_2$  run.

To find more shifts in the climate time series, we have to reduce our detection threshold level, which amounts to picking up less obvious abrupt changes than those found for  $C_{veg}$  (e.g. Figure 4). We find shifts in the temperature time series with a detection threshold of 0.3, and in the rainfall time series with a detection threshold of 0.2. Figure S2 shows a map of shifts with these detection values. Examples of these shifts are shown in Figure S3, which serve to



illustrate that these detection levels are too low to find shifts that are obviously abrupt.

There is very little spatial overlap between where  $C_{veg}$  abrupt shifts are detected and where rainfall or temperature shifts are detected (with the lowered detection thresholds). When comparing  $C_{veg}$  to temperature and precipitation within the four runs, the largest overlap of the eight resultant combinations, is that in the 3.5K, A1B  $CO_2$  simulation, where 18.1% of  $C_{veg}$  abrupt shifts coincide spatially with detected rainfall shifts. In 3.5K, constant  $CO_2$ ,  $C_{veg}$  and rainfall shifts have 6.9% spatial overlap. In 7.1K, A1B  $CO_2$ ,  $C_{veg}$  and rainfall shifts have 6.4% overlap. The other five combinations have less than 4% overlap. This indicates that the majority of  $C_{veg}$  abrupt shifts are not due to corresponding shifts in climate drivers.

### 3.6 | Early warning signals of $C_{veg}$ abrupt shifts

The results of looking for early warning signals of tipping point dynamics before the 'traditional' abrupt shifts in  $C_{veg}$  time series (both increases and decreases), for all four of the configurations, are summarized in Figure 6. This shows histograms of Kendall  $\tau$  values (measuring the tendency of the indicator time series; see Section 2). The top row is for lag-1 autocorrelation (AR(1)) as an indicator, the bottom row for variance, and the columns are the four different configurations. The blue histograms are for traditional increasing abrupt

shifts and the red histograms for traditional decreasing abrupt shifts. We note that there were no traditional decreasing abrupt shifts for the 3.5K or 7.1K, A1B  $CO_2$  configurations.

We find that 81.0% of the increasing abrupt shifts have increasing AR(1) values (3.5K, const.  $CO_2$ : 30.8%, 3.5K, A1B  $CO_2$ : 95.0%, 7.1K, const.  $CO_2$ : 90.1%, 7.1K, A1B  $CO_2$ : 42.9%) and 73.9%, increasing variance values (30.8%, 71.4%, 95.8%, 45.6%). This is compared with 59.4% (3.5K, const.  $CO_2$ : 60.8%, 7.1K, const.  $CO_2$ : 57.1%) and 49.1% (48.3%, 50.5%) for decreasing abrupt shifts respectively. For a true early warning signal, we would expect both increasing AR(1) and variance values. This is true of 70.0% of the increasing abrupt shift time series (3.5K, const.  $CO_2$ : 23.1%, 3.5K, A1B  $CO_2$ : 71.4%, 7.1K, const.  $CO_2$ : 89.2%, 7.1K, A1B  $CO_2$ : 38.9%). For decreasing abrupt shifts, this is only true of 49.1% of time series (3.5K, const.  $CO_2$ : 48.3%, 7.1K, const.  $CO_2$ : 50.5%). Kolmogorov–Smirnov tests on increasing and decreasing abrupt shifts for both AR(1) and variance show that in all four cases, the distributions are not normal ( $p < .001$ ), which would be expected with no early warning. The distribution of the AR(1) values for increasing abrupt shifts are strongly negatively skewed (-1.16), with moderate skewness also observed for the variance values (-0.54). Skewness for decreasing abrupt shifts are less (-0.17 and 0.10 respectively). Overall we find that increasing  $C_{veg}$  abrupt shifts show greater prospects for early warning signals than decreasing ones, and with the exception of the 3.5K, constant  $CO_2$  run (which only contains 13 examples of increasing abrupt shifts), those prospects are quite promising.

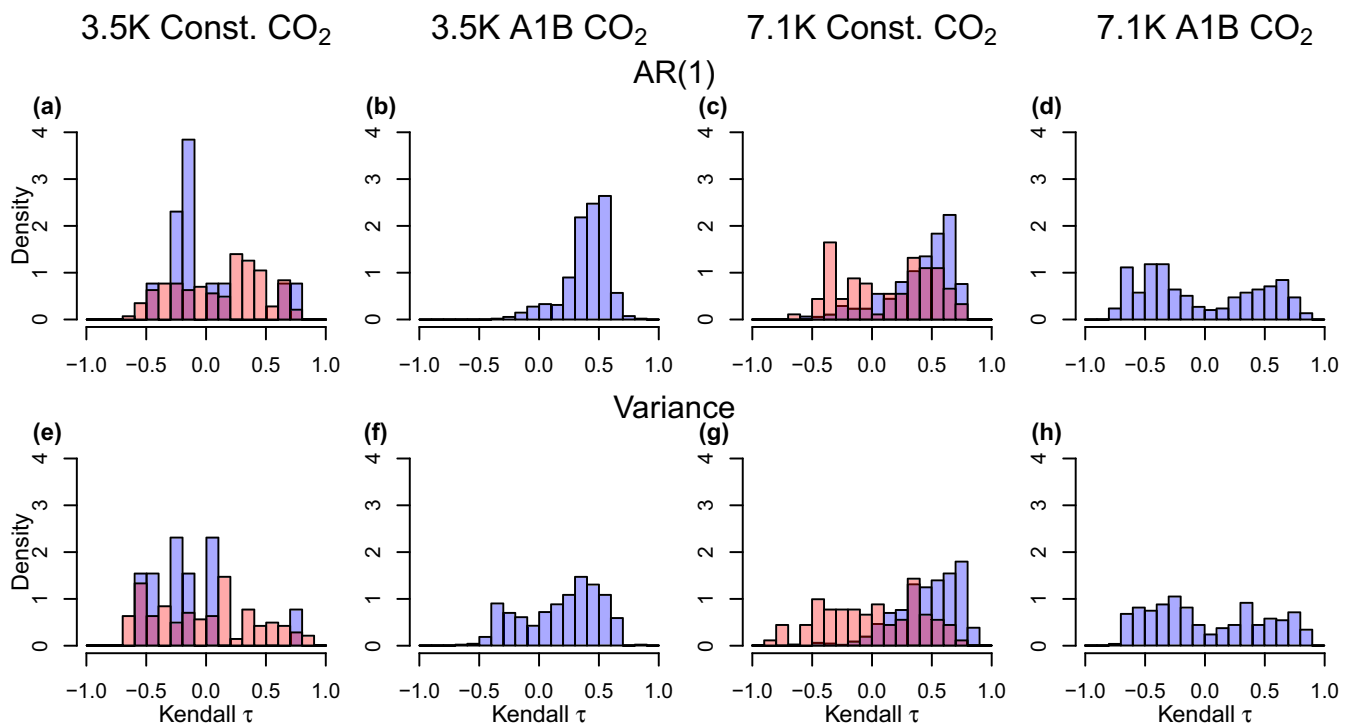


**FIGURE 6** Histogram of Kendall  $\tau$  values of (a–d) AR(1) and (e–h) variance time series calculated from grid box  $C_{veg}$  time series for tipping points classified as (blue) traditional,  $D > 0$ ,  $AS > 0$  and (red) traditional,  $D < 0$ ,  $AS < 0$  with a detection rating over 0.4 in JULES configurations (a, e) 3.5K, constant  $CO_2$ , (b, f) 3.5K, A1B  $CO_2$ , (c, g) 7.1K, constant  $CO_2$  and (d, h) 7.1K, A1B  $CO_2$ . For comparison, the density (such that the summed areas of the bars equals 1 for each configuration) rather than the counts are shown due to the variation in the number of grid boxes in each classification

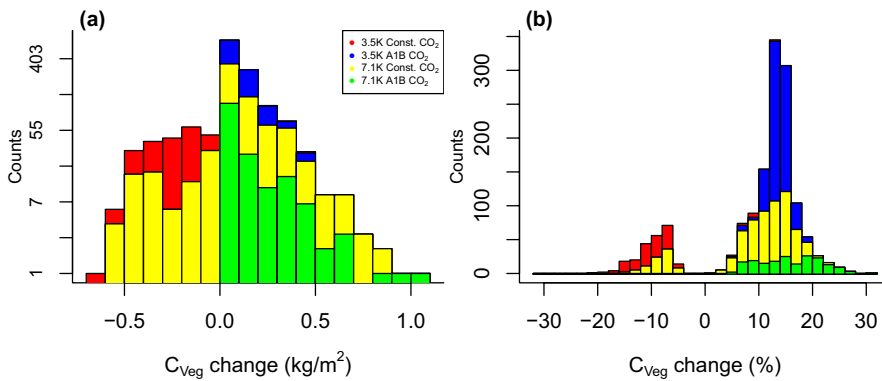


**FIGURE 7** Difference in  $C_{veg}$  time series due to the traditional abrupt shifts within them. (a) Difference in the 5 year means post- and pre-abrupt shift and (b) these differences as a percentage of the starting  $C_{veg}$  (the first 5 years of the time series). Note the log scale on some axes

### 3.7 | Size of the abrupt shifts

Given the surprising number of abrupt shifts it is interesting to consider how large they are. We reiterate here that we have already excluded changes which are less than  $0.01 \text{ kg/m}^2$ . Figure 7 shows the change in  $C_{veg}$  across the two classes of traditional abrupt shift (those we measure early warning signals for). These are calculated as the difference between 5 year means; 5 years before and after the year the shift was detected. In the rare case that the shift was detected less than 5 years before the end of the run, we take values up to the end of the run. Note that these differences are associated with the abrupt shift itself rather than the overall change in  $C_{veg}$  across the run.

In Figure 7a, we can see that abrupt shifts are capable of increasing  $C_{veg}$  by more than  $1 \text{ kg/m}^2$  and decreases of more than  $0.5 \text{ kg/m}^2$ . There are 25 grid boxes that have  $C_{veg}$  increases of more than  $0.5 \text{ kg/m}^2$  across the detected abrupt shift within them, and seven that have decreases of more than  $0.5 \text{ kg/m}^2$ . The large increases come from the 7.1K runs, whereas the large decreases come from the constant  $\text{CO}_2$  runs. Given that GB is dominated by grasslands rather than woodland these are significant changes in  $C_{veg}$ .

Because we find a range of baseline  $C_{veg}$  (Figure 2) and of changes in  $C_{veg}$  (Figure 3) and thus a wide range of differences in  $C_{veg}$  across the runs, we decided to look at the percentage change in  $C_{veg}$  across the abrupt shift (Figure 7b), defined as a percentage of the starting value of  $C_{veg}$  (mean first 5 years). We find that increasing abrupt shifts account for a mean 13.4% increase on the starting value of  $C_{veg}$ . Decreasing abrupt shifts account for a mean 9.6% decrease relative to the starting  $C_{veg}$ . A caveat here is that  $C_{veg}$  values are lower bounded at 0 and as such decreases are bounded by how much starting vegetation there is to begin with.

## 4 | DISCUSSION

### 4.1 | Differences in results between configurations

We find differences in how  $C_{veg}$  changes over the 21st century and what classification of abrupt shift we observe between our four configurations. As Figure 3 shows, with increasing  $\text{CO}_2$  and climate change,  $C_{veg}$  is generally projected to increase, whilst climate change

alone forces high losses of  $C_{veg}$  in certain areas. This is consistent with a strong  $\text{CO}_2$  fertilization effect on plant growth in the JULES-TRIFFID model. This manifests somewhat in the classes of abrupt shifts detected in  $C_{veg}$  (Figure 5), where there are many abrupt shifts involving increases in  $C_{veg}$  (Table 1). However, this is also true under 7.1K climate sensitivity when  $\text{CO}_2$  is held constant. That pattern of climate change alone causes abrupt increases in  $C_{veg}$ , particularly in the highlands of Scotland in this model.

In simulations without increases in  $\text{CO}_2$ , we find more increasing abrupt shifts in the 7.1K climate sensitivity simulation, with less decreasing shifts when compared with the 3.5K simulation. This could suggest that in some places, the vegetation growth is limited by the smaller temperature increases in the 3.5K simulation. In simulations where  $\text{CO}_2$  changes are included, we see more increasing abrupt shifts in the 3.5K simulation, despite seeing more increases in  $C_{veg}$  in the 7.1K run. However, the increases in  $C_{veg}$  in the 7.1K run are not detected by our algorithm, suggesting that they are non-abrupt increases.

### 4.2 | Mechanisms for abrupt shifts found in $C_{veg}$ time series

We examined several possible causes of the abrupt shifts in  $C_{veg}$ . Having established that they are not generally due to abrupt shifts in climate drivers, we also considered whether the spatial patterns of changes in temperature or rainfall bore any relation to the location of abrupt shifts. We calculated the first four principal components of temperature and rainfall change (Figure S4), but none of these patterns clearly relate to the patterns of abrupt shifts (Figure 5).

Hence we focused attention on the equations and parameters of the vegetation and soil models, looking for non-linear dynamics or threshold behaviour within them that could give rise to abrupt shifts in response to smooth forcing. Here we note that bifurcations, where there is a loss of stability in the state of a system such that the system moves to an alternative stable state, do not necessarily have to occur to observe abrupt shifts and detect early warning signals of them (Kéfi, Dakos, Scheffer, Van Nes, & Rietkerk, 2013).

In our vegetation model, there are non-linearities in the equations governing the calculation of  $C_{veg}$ , detailed in Appendix S1,

which could contribute to abrupt shifts. Net primary productivity (NPP), which is converted into  $C_{\text{Veg}}$ , increases (nonlinearly) with increasing atmospheric  $\text{CO}_2$  and temperature. There is a non-linear relation between  $C_{\text{Veg}}$  and the balanced leaf area index (LAI), which a PFT would have in full leaf. Furthermore, depending on LAI,  $C_{\text{Veg}}$  is fractionally assigned in a piecewise linear way either to grow the plant and store carbon (low balanced LAI), or to spread the plant (high LAI). Together these equations can sometimes give rise to self-amplifying responses, for example, escalating growth at low LAI, which can contribute to abrupt increases in  $C_{\text{Veg}}$ .

We undertook a search for spatial correlation between model soil parameters and the occurrence of abrupt shifts. We found that two soil properties, critical soil moisture content (CSMC) and heat capacity are linked to the spatial occurrence of abrupt shifts and anti-correlated with each other. These are fixed parameters linked to the type of soil prescribed at each location in the model. In particular, CSMC determines the steepness of a piecewise linear relationship between productivity and soil moisture content (Cox et al., 1999). In particular, low CSMC can create a threshold behaviour that could explain why low critical values are associated with traditional, decreasing abrupt shifts (Figure 8 for the 3.5K constant  $\text{CO}_2$  scenario). Lower CSMC values mean that there is a steeper decline in photosynthesis between this value and the moisture content value that causes the plant to wilt (where photosynthesis does not occur). If climate changes drives soil moisture content down into this range, then there is the potential for an abrupt drop in photosynthesis and  $C_{\text{Veg}}$ . Constant  $\text{CO}_2$  scenarios give the greatest potential for these drought thresholds to be transgressed because there is no physiological effect of elevated  $\text{CO}_2$  increasing plant water use efficiency. With higher CSMC values, this problem is less acute—the decrease in productivity with drying is less extreme and so is less likely to cause an abrupt shift.

### 4.3 | Explaining the early warning signals of $C_{\text{Veg}}$ abrupt shifts

To attempt to determine why we find more early warning signals of the abrupt shifts in certain cases but not in others, namely in

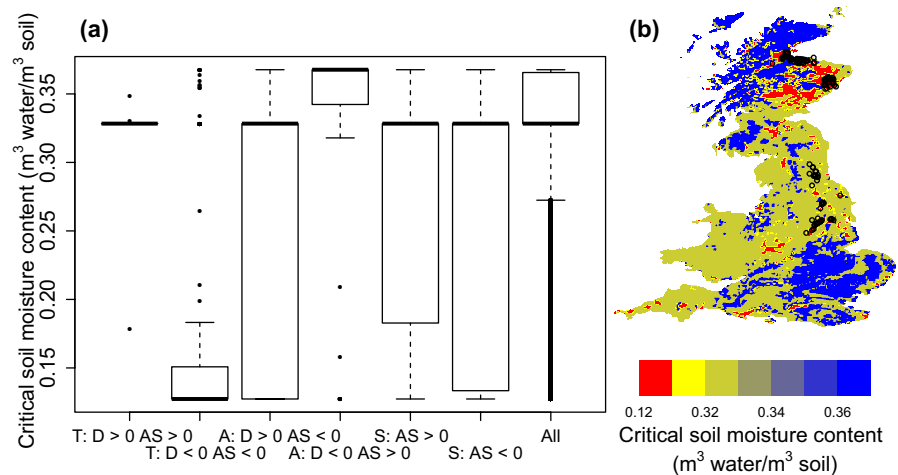
increasing shifts rather than decreasing, we considered the dominant PFTs in each grid box where shifts are found. Previous work has shown that it is difficult to get early warning signals of dieback from broadleaf tree fraction in the Amazon rainforest (Boulton, Good, & Lenton, 2013). This is partially due to the low variability of long lasting broadleaf trees when compared with the variability associated with grasses (particularly C3 grasses in this instance). We looked for correlations between the tendencies of the early warning indicators (Figure 6) and the grass fraction or tree fraction in grid boxes; however, we were unable to find anything significant in these results.

Instead, having established that at least some decreasing shifts are associated with soil moisture thresholds (Figure 8), we reason that these would be unlikely to show early warning signals because they are not due to a change in feedbacks internal to the vegetation model. In contrast, increases in NPP and  $C_{\text{Veg}}$  driven by increasing  $\text{CO}_2$  and temperature, can be self-amplifying (equations in Appendix S1). In particular, small plants with low LAI can grow at an accelerating rate. As well as potentially giving rise to abrupt increases in  $C_{\text{Veg}}$ , this change in internal feedbacks is in the direction that should give rise to early warning signals.

### 4.4 | Limitations and suggestions for future work

This study considers only one climate (general circulation) model and one land surface model. Given that the structurally different instances of the climate model (the different climate sensitivities) give rise to different results for the number and location of abrupt shifts in the same land surface model, we can expect that other climate projections with other climate models would give different results again. Equally, given that the results are sensitive to switching on and off the uncertain sensitivity of vegetation to increasing  $\text{CO}_2$ , we can expect that different land surface models would give different results again. In our chosen vegetation model, the non-linear amplifier of escalating growth at low LAI seems physiologically reasonable—as plants grow there is usually a phase of accelerating growth. Equally, the representation that some soil types dry out rapidly causing wilting seems pedologically reasonable. Nevertheless, it

**FIGURE 8** The critical soil moisture content (CSMC) values for each grid box, supplied as an input to JULES. (a) Box and whisker plots show the distribution of CSMC for grid boxes that detected each of the abrupt shifts in the 3.5K constant  $\text{CO}_2$  simulations (and all grid boxes together, regardless of abrupt shift detection). (b) A map of these critical values is also shown, with open black circles denoting the location of the traditional decreasing abrupt shifts (T:  $D < 0$  AS  $< 0$ )



would be interesting for future work to test whether other land surface models with different equations also give rise to abrupt shifts. The chosen land surface model is missing several potential sources of abrupt changes—in particular climate-sensitive disturbance factors, such as fire and disease vectors—meaning it may underestimate the potential for abrupt shifts. For these reasons, we view the present results as ‘projections’, which illustrate the potential for abrupt shifts in GB vegetation carbon under climate change, and the potential for them to show early warning signals. Our results should not be viewed as ‘predictions’ of where and when such abrupt shifts will occur.

## 5 | SUMMARY

To summarize, we have shown results from four different model configurations that show abrupt shift behaviour in vegetation carbon due to climate change (with or without CO<sub>2</sub> change) at small spatial scales across GB. We have identified the types of shifts that occur and have shown that these generally appear not to be linked to abrupt shifts in climate. Detectable shifts in rainfall or temperature time series are modest, not really abrupt, and rarely spatially overlapping with the numerous and scattered abrupt shifts in vegetation carbon. A subset of abrupt shifts that involve decreases in vegetation carbon can be linked to a high sensitivity of photosynthesis to soil moisture content in those locations. For the ‘traditional’ abrupt shifts that go in the same direction as overall trends in vegetation carbon, we find evidence of early warning signals consistent with tipping point dynamics, particularly for abrupt increases in vegetation carbon within an overall increasing trend. These abrupt shifts and the associated early warning signals can be linked to self-amplifying non-linear dynamics in the equations describing changes in vegetation carbon. Many of the abrupt shifts are non-trivial in size with large shifts detected in both directions relative to the amount of C<sub>veg</sub> that is stored.

## ACKNOWLEDGEMENTS

This work was funded by the NERC Valuing Nature programme, grant number NE/P007880/1 and the Leverhulme Trust, grant number RPG-2018-046. The authors acknowledge use of the Monsoon2 system, a collaborative facility supplied under the Joint Weather and Climate Research Programme, a strategic partnership between the Met Office and NERC. We also thank the Land, Environment, Economics and Policy (LEEP) Institute at the University of Exeter, and Dr Anna Harper and Dr Angela Gallego-Sala for their inputs.

## DATA AVAILABILITY STATEMENT

The parameter values used for JULES are available from the suite u-ao645 and branch ‘transient\_25km\_drive’ on the Rosie repository: <https://code.metoffice.gov.uk/trac/roses-u> (registration required). The modelled output of this study is openly available in Boulton and Ritchie (2020). The climate data are available at Hadley Centre for Climate Prediction and Research (2014).

## ORCID

Chris A. Boulton  <https://orcid.org/0000-0001-7836-9391>

Paul D. L. Ritchie  <https://orcid.org/0000-0002-7649-2991>

Timothy M. Lenton  <https://orcid.org/0000-0002-6725-7498>

## REFERENCES

- Allen, C. D., Macalady, A. K., Chenchouni, H., Bachelet, D., McDowell, N., Vennetier, M., ... Cobb, N. (2010). A global overview of drought and heat-induced tree mortality reveals emerging climate change risks for forests. *Forest Ecology and Management*, 259(4), 660–684. <https://doi.org/10.1016/j.foreco.2009.09.001>
- Alley, R. B. (2000). Ice-core evidence of abrupt climate changes. *Proceedings of the National Academy of Sciences of the United States of America*, 97(4), 1331–1334. <https://doi.org/10.1073/pnas.97.4.1331>
- Alley, R. B., Marotzke, J., Nordhaus, W. D., Overpeck, J. T., Peteet, D. M., Pielke, R. A., ... Wallace, J. M. (2003). Abrupt climate change. *Science*, 299(5615), 2005–2010. <https://doi.org/10.1126/science.1081056>
- Bentz, B. J., Régnière, J., Fettig, C. J., Hansen, E. M., Hayes, J. L., Hicke, J. A., ... Seybold, S. J. (2010). Climate change and bark beetles of the western United States and Canada: Direct and indirect effects. *BioScience*, 60(8), 602–613. <https://doi.org/10.1525/bio.2010.60.8.6>
- Best, M. J., Pryor, M., Clark, D. B., Rooney, G. G., Essery, R. L. H., Ménard, C. B., ... Harding, R. J. (2011). The Joint UK Land Environment Simulator (JULES), model description – Part 1: Energy and water fluxes. *Geoscientific Model Development*, 4(3), 677–699. <https://doi.org/10.5194/gmd-4-677-2011>
- Boulton, C. A., Good, P., & Lenton, T. M. (2013). Early warning signals of simulated Amazon rainforest dieback. *Theoretical Ecology*, 6(3), 373–384. <https://doi.org/10.1007/s12080-013-0191-7>
- Boulton, C. A., & Lenton, T. M. (2019). A new method for detecting abrupt shifts in time series [version 1; peer review: 2 approved with reservations]. *F1000Research*, 8, 746. <https://doi.org/10.12688/f1000research.19310.1>
- Boulton, C. A., & Ritchie, P. D. (2020). Modelled vegetation carbon, temperature and rainfall for Great Britain 1997–2099 under four climate and CO<sub>2</sub> scenarios. *NERC Environmental Information Data Centre*, <https://doi.org/10.5285/f493ad5c-585c-475d-a374-2f77b5866bc4>
- Carpenter, S. R., & Kinne, O. (2003). *Regime shifts in lake ecosystems: Pattern and variation* (Vol. 15). Oldendorf/Luhe, Germany: International Ecology Institute.
- Clark, D. B., Mercado, L. M., Sitch, S., Jones, C. D., Gedney, N., Best, M. J., ... Cox, P. M. (2011). The Joint UK Land Environment Simulator (JULES), model description – Part 2: Carbon fluxes and vegetation dynamics. *Geoscientific Model Development*, 4(3), 701–722. <https://doi.org/10.5194/gmd-4-701-2011>
- Cox, P. M. (2001). Description of the ‘TRIFFID’ dynamical global vegetation model. *Hadley Centre Technical Note*, 24.
- Cox, P. M., Betts, R. A., Bunton, C. B., Essery, R. L. H., Rowntree, P. R., & Smith, J. (1999). The impact of new land surface physics on the GCM simulation of climate and climate sensitivity. *Climate Dynamics*, 15(3), 183–203. <https://doi.org/10.1007/s003820050276>
- Cox, P. M., Betts, R., Jones, C., Spall, S., & Totterdell, I. (2001). Modelling vegetation and the carbon cycle as interactive elements of the climate system. *Hadley Centre Technical Note*, 23.
- Dakos, V., Scheffer, M., van Nes, E. H., Brovkin, V., Petoukhov, V., & Held, H. (2008). Slowing down as an early warning signal for abrupt climate change. *Proceedings of the National Academy of Sciences of the United States of America*, 105(38), 14308–14312. <https://doi.org/10.1073/pnas.0802430105>
- Davis, K. T., Dobrowski, S. Z., Higuera, P. E., Holden, Z. A., Veblen, T. T., Rother, M. T., ... Maneta, M. P. (2019). Wildfires and climate change push low-elevation forests across a critical climate threshold for tree regeneration. *Proceedings of the National Academy of Sciences*

- of the United States of America, 116(13), 6193–6198. <https://doi.org/10.1073/pnas.1815107116>
- Drijfhout, S., Bathiany, S., Beaulieu, C., Brovkin, V., Claussen, M., Huntingford, C., ... Swingedouw, D. (2015). Catalogue of abrupt shifts in Intergovernmental Panel on Climate Change climate models. *Proceedings of the National Academy of Sciences of the United States of America*, 112(43), E5777–E5786. <https://doi.org/10.1073/pnas.1511451112>
- Evans, P. M., Newton, A. C., Cantarello, E., Martin, P., Sanderson, N., Jones, D. L., ... Fuller, L. (2017). Thresholds of biodiversity and ecosystem function in a forest ecosystem undergoing dieback. *Scientific Reports*, 7(1), 6775. <https://doi.org/10.1038/s41598-017-06082-6>
- Gallego-Sala, A. V., & Prentice, I. C. (2012). Blanket peat biome endangered by climate change. *Nature Climate Change*, 3, 152–155. <https://doi.org/10.1038/nclimate1672>
- Hadley Centre for Climate Prediction and Research. (2014). *UKCP09: Met Office HadRM3-PPE UK model runs*. Retrieved from <http://catalogue.ceda.ac.uk/uuid/465ecd8a305ffb9df2bd8b54cada669f>
- Harper, A. B., Wiltshire, A. J., Cox, P. M., Friedlingstein, P., Jones, C. D., Mercado, L. M., ... Duran-Rojas, C. (2018). Vegetation distribution and terrestrial carbon cycle in a carbon cycle configuration of JULES4.6 with new plant functional types. *Geoscientific Model Development*, 11(7), 2857–2873. <https://doi.org/10.5194/gmd-11-2857-2018>
- Held, H., & Kleinen, T. (2004). Detection of climate system bifurcations by degenerate fingerprinting. *Geophysical Research Letters*, 31(23), <https://doi.org/10.1029/2004gl020972>
- Hirota, M., Holmgren, M., Van Nes, E. H., & Scheffer, M. (2011). Global resilience of tropical forest and savanna to critical transitions. *Science*, 334(6053), 232–235. <https://doi.org/10.1126/science.1210657>
- Hoffman, W. A., Marchin, R. M., Abit, P., & Lau, O. L. (2011). Hydraulic failure and tree dieback are associated with high wood density in a temperate forest under extreme drought. *Global Change Biology*, 17(8), 2731–2742. <https://doi.org/10.1111/j.1365-2486.2011.02401.x>
- Ibáñez, I., Clark, J. S., Dietze, M. C., Feeley, K., Hersh, M., LaDeau, S., ... Wolosin, M. S. (2006). Predicting biodiversity change: Outside the climate envelope, beyond the species–area curve. *Ecology*, 87(8), 1896–1906. [https://doi.org/10.1890/0012-9658\(2006\)87\[1896:PB-COTC\]2.0.CO;2](https://doi.org/10.1890/0012-9658(2006)87[1896:PB-COTC]2.0.CO;2)
- Kéfi, S., Dakos, V., Scheffer, M., Van Nes, E. H., & Rietkerk, M. (2013). Early warning signals also precede non-catastrophic transitions. *Oikos*, 122(5), 641–648. <https://doi.org/10.1111/j.1600-0706.2012.20838.x>
- Kéfi, S., Holmgren, M., & Scheffer, M. (2016). When can positive interactions cause alternative stable states in ecosystems? *Functional Ecology*, 30(1), 88–97. <https://doi.org/10.1111/1365-2435.12601>
- Kurz, W. A., Dymond, C. C., Stinson, G., Rampley, G. J., Neilson, E. T., Carroll, A. L., ... Safranyik, L. (2008). Mountain pine beetle and forest carbon feedback to climate change. *Nature*, 452(7190), 987. <https://doi.org/10.1038/nature06777>
- Lenton, T. M. (2013). Environmental tipping points. *Annual Review of Environment and Resources*, 38(1), 1–29. <https://doi.org/10.1146/annurev-environ-102511-084654>
- Lenton, T. M., Held, H., Kriegler, E., Hall, J. W., Lucht, W., Rahmstorf, S., & Schellnhuber, H. J. (2008). Tipping elements in the Earth's climate system. *Proceedings of the National Academy of Sciences of the United States of America*, 105(6), 1786–1793. <https://doi.org/10.1073/pnas.0705414105>
- Martin, P., Newton, A. C., Cantarello, E., & Evans, P. M. (2017). Analysis of ecological thresholds in a temperate forest undergoing dieback. *PLoS ONE*, 12(12), e0189578. <https://doi.org/10.1371/journal.pone.0189578>
- Murphy, J. M., Sexton, D., Jenkins, G., Boorman, P., Booth, B., Brown, C., ... Kendon, E. (2009). *UK climate projections science report: Climate change projections* (pp. 21–35) Exeter: Met Office Hadley Centre.
- Ratajczak, Z., Carpenter, S. R., Ives, A. R., Kucharik, C. J., Ramiadantsoa, T., Stegner, M. A., ... Turner, M. G. (2018). Abrupt change in ecological systems: Inference and diagnosis. *Trends in Ecology & Evolution*, 33(7), 513–526. <https://doi.org/10.1016/j.tree.2018.04.013>
- Scheffer, M. (2009). *Critical Transitions in Nature and Society* (Vol. 16). Princeton, NJ: Princeton University Press.
- Scheffer, M., Bascompte, J., Brock, W. A., Brovkin, V., Carpenter, S. R., Dakos, V., ... Sugihara, G. (2009). Early-warning signals for critical transitions. *Nature*, 461, 53. <https://doi.org/10.1038/nature08227>
- Scheffer, M., Carpenter, S., Foley, J. A., Folke, C., & Walker, B. (2001). Catastrophic shifts in ecosystems. *Nature*, 413(6856), 591–596. <https://doi.org/10.1038/35098000>
- Scheffer, M., & Jeppesen, E. (2007). Regime shifts in shallow lakes. *Ecosystems*, 10(1), 1–3. <https://doi.org/10.1007/s10021-006-9002-y>
- Staver, A. C., Archibald, S., & Levin, S. A. (2011). The global extent and determinants of savanna and forest as alternative biome states. *Science*, 334(6053), 230. <https://doi.org/10.1126/science.1210465>
- Thomas, C. D., Cameron, A., Green, R. E., Bakkenes, M., Beaumont, L. J., Collingham, Y. C., ... Williams, S. E. (2004). Extinction risk from climate change. *Nature*, 427(6970), 145. <https://doi.org/10.1038/nature02121>
- Zhu, Z., Piao, S., Myneni, R. B., Huang, M., Zeng, Z., Canadell, J. G., ... Zeng, N. (2016). Greening of the Earth and its drivers. *Nature Climate Change*, 6(8), 791–795. <https://doi.org/10.1038/nclimate3004>

## SUPPORTING INFORMATION

Additional supporting information may be found online in the Supporting Information section.

**How to cite this article:** Boulton CA, Ritchie PDL, Lenton TM. Abrupt changes in Great Britain vegetation carbon projected under climate change. *Glob Change Biol*. 2020;00:1–13. <https://doi.org/10.1111/gcb.15144>